



# Exploring potential application of novel urease-producing bacterium for sustainable soil stabilization via microbially induced calcium carbonate precipitation

Achuth Jayakrishnan<sup>1\*</sup>, Abhijith Kozhipally<sup>1</sup> and Mahenthiran Ramasamy<sup>2</sup>

<sup>1</sup>Department of Microbiology, Hindusthan College of Arts and Science, Avinashi Rd, behind Nava India, Udayampalayam, 641028, Coimbatore, Tamil Nadu, India.

<sup>2</sup>Department of Microbiology, Dr. NGP Arts & Science College, Coimbatore, Tamil Nadu, India. \*Author for correspondence. E-mail: achuaj08@gmail.com

**ABSTRACT.** Microbially induced calcium carbonate precipitation (MICP) is a sustainable process involving microbial-mediated calcium carbonate precipitation with applications in geotechnical engineering, construction, and environmental remediation. Soil samples from paddy fields were screened for ureolytic bacteria, and the isolate with the highest urease activity was identified as *Bacillus tequilensis* strain AK1 via 16S rRNA sequencing. The strain achieved a maximum CaCO<sub>3</sub> precipitation of 23.00 mg mL<sup>-1</sup> on Day 20 in broth media and a calcite precipitation zone diameter of 17.05 mm in agar media. Bioconsolidation of soil with *Bacillus tequilensis* strain AK1 showed significant enhancements in soil properties. Retention time increased to 164 sec compared to 15 sec in controls, while penetration distance decreased to 43 mm, a substantial reduction from 483 mm in untreated samples. Water absorption was notably reduced to 7.4%, compared to 66.5% in controls. These findings confirm that microbial calcite precipitation effectively aggregates particles and fills pore spaces, improving soil structural integrity. This study highlights the potential of *Bacillus tequilensis* strain AK1 for sustainable bioconsolidation, offering a promising solution for soil stabilization, construction, and environmental remediation.

**Keywords:** Microbially induced calcium carbonate precipitation; urease-producing bacteria; bioconsolidation; bioremediation; calcium carbonate.

Received on February 25, 2025

Accepted on June 02, 2025

## Introduction

Calcium carbonate (CaCO<sub>3</sub>) is extensively utilized crucial material with significant utility across various sectors, such as construction, papermaking, and as a source of calcium supplementation. (Hammes & Verstraete, 2002). The exploration of environmentally sustainable techniques for the biosynthesis and application of calcium carbonate has been explored extensively and this has progressively led to the culmination of microbially induced calcium carbonate precipitation (MICP). This technique utilizes the enzymatic activity of urease-producing bacteria facilitating calcium carbonate precipitation through biochemical processes that occur under controlled environmental conditions (Weiner, 2008). Among the diverse group of microorganisms responsible for calcite precipitation, urease-producing bacteria such as *Bacillus*, *Sporosarcina*, and *Pseudomonas*, are of particular interest in this biomineralization processes. These bacteria possess highly robust metabolic systems that enable the hydrolysis of urea leading to the efficient precipitation of calcium carbonate (CaCO<sub>3</sub>) (Achal et al., 2009). The calcite formed serves as a cementing agent, promoting the aggregation of soil particles and enhancing their overall structural stability and integrity of resulting material.

The process of MICP encompasses two primary mechanisms: biologically controlled precipitation and biologically induced precipitation. The precipitation process in controlled mechanisms is regulated by microbial cells that modulate the nucleation and controlled particle growth. Conversely, biologically induced precipitation is largely dependent on external environmental conditions, which increases more susceptible to changes in pH, calcium ion levels, and the availability of nucleation sites (Vekariya & Pitroda, 2013).

The efficiency of MICP is determined by a variety of factors including the metabolic activity of the bacteria, nutrient availability and environmental conditions. The catalytic activity of urease is influenced by the metabolic state of bacterial cells and the presence of nickel ions which act as critical cofactors (Park &

Hausinger, 1995). Moreover, the characteristics of calcite crystal formation, including size and distribution are dependent on the levels of calcium and carbonate ions, as well as the pH of the medium through collectively modulating crystal nucleation and growth (Qian et al., 2010).

MICP exhibits broad and wide range of applications underlining its versatile potential in a variety of scientific, environmental, and engineering sectors. In environmental remediation, MICP has shown substantial efficacy for immobilizing heavy metals and radionuclides within soil, thereby significantly reducing their bioavailability. The capacity of calcite to incorporate toxic ions such as lead, cadmium, and uranium into their crystal lattice and thereby diminishing its mobility and bioavailability contributes in effective mitigation of environmental contamination (Mitchell & Ferris, 2005). Moreover, MICP has also been explored for its potential to facilitate carbon sequestration, wherein the precipitation of calcium carbonate provides a stable and long-term mechanism for the capture and storage of atmospheric CO<sub>2</sub> (Ghosh et al., 2019).

MICP has been employed as an effective soil stabilization technique within geotechnical engineering, where the precipitation of calcium carbonate decreases porosity and enhances its load-bearing capacity (DeJong et al., 2010). This approach has demonstrated considerable efficacy in reducing soil liquefaction, a phenomenon that contributes to severe infrastructure damage during seismic events (Hammes & Verstraete, 2002). In the construction industry, MICP has been investigated for its ability to seal microcracks in concrete, which serves to improve their structural integrity and operational lifespan (Wang et al., 2014). This biotechnological intervention presents a green alternative to conventional chemical sealants that are frequently associated with adverse environmental impacts.

While MICP holds significant promise, its practical implementation is impeded by several technical and operational challenges related to scalability and efficiency. A primary concern in scaling the process is the production of urease and bacterial transport through soil matrices, which are influenced by the availability of nutrients and environmental constraints (Dhami et al., 2013). Additionally, the durability and stability of biocemented materials under varying environmental conditions are still under active exploration.

Soil samples were collected and screened for urease-producing bacteria, with organism selected based on its urease activity. The strain was cultured in nutrient-rich media and evaluated for its ability to precipitate calcium carbonate under controlled laboratory conditions. The bacterial isolate was applied to soil and sand samples to assess its bioconsolidation potential. Various analyses, including penetration tests, water absorption studies, and retention time measurements, were performed to evaluate the mechanical and physicochemical properties of bioconsolidated samples. Additionally, the cell surface hydrophobicity and adhesion properties of the bacterial isolate were examined to understand their role in calcite formation and soil stabilization. This study aims to provide insights into optimizing MICP for sustainable applications in geotechnical engineering and environmental management.

## Materials and methods

### Collection of Samples

Samples from the soil were collected at a depth of 5-10 cm from various paddy field locations in Nilambur, Kerala, India. The samples were collected using sterile tools, and the samples were transferred to sterile plastic containers, and immediately stored in an icebox for transportation to the laboratory for further examination.

### Isolation of urease-producing bacteria

Soil samples were screened for bacteria exhibiting high urease activity and capable of calcite precipitation. Soil (1 g) was transferred into 50 mL of enrichment medium (10 g mL<sup>-1</sup> yeast extract (YE), 1 M urea, 152 mM ammonium sulfate, and 100 mM sodium acetate; pH 7.0), which was prepared in 250 mL Erlenmeyer flasks. The medium was subjected to sterilization at 121 °C for 15 min, and filter-sterilized urea was incorporated into the medium post-autoclaving to avoid degradation. The flasks were incubated at 28 °C for 36 hours at 130 rpm.

The enrichment cultures were serially diluted and plated onto nutrient agar (NA) plates containing 8% (w/v) filter-sterilized urea, in order to isolate pure colonies. The plates were incubated at 28 °C for 48 hours, following which phenolphthalein, a pH indicator, was carefully applied to the colony surfaces to assess metabolic activity of the isolates. Colonies exhibiting a pinkish appearance were selectively transferred to enrichment medium and cultured as mentioned above for subsequent characterization (Al-Thawadi & Cord-Ruwisch, 2012).

### Molecular characterization of the urease producing bacteria

The molecular identification of the bacterial isolates was performed through 16S rRNA gene sequencing. Genomic DNA was extracted from the bacterial isolates, followed by PCR amplification of the 16S rRNA gene with universal primers. The amplified 16S rRNA gene was sequenced in both the forward and reverse directions. The resulting sequences were then subjected to a BLAST (Basic Local Alignment Search Tool) search against the NCBI nucleotide database to identify the bacterial species with the highest sequence similarity. The sequence similarity percentage was calculated, and the validated sequences were subsequently deposited in the NCBI GenBank database to acquire corresponding accession number (Sujatha et al., 2012).

### Assessment of Calcium Carbonate Precipitation

#### Precipitation in broth Media

Calcium carbonate ( $\text{CaCO}_3$ ) precipitation was quantified following a modified procedure derived from Krishnapriya et al., (2015). Bacterial culture was inoculated in 25 mL of B4 medium (containing 0.4% yeast extract, 1% dextrose, and 0.25% calcium acetate, pH 8.0) and incubated for 10 days with continuous shaking 200 rpm at 27°C. The culture was distributed into six aliquots of 2.5 mL each and subjected to centrifugation at 5000 rpm for 3 min. The supernatant, containing bacterial cells was discarded, while the pellet, consisting of  $\text{CaCO}_3$  crystals, was resuspended in 2 mL of calcium hypochlorite-saturated Milli-Q water and vortexed for 1 min. The suspension was filtered through Whatman No. 1 filter paper and washed twice with distilled water.

For the control, bacteria was inoculated into B4 medium without calcium acetate, with all subsequent steps identical to those in the experimental procedure. The precipitation kinetics of  $\text{CaCO}_3$  were assessed over a 10-day period, with sampling conducted every 2 days to monitor the process. The mass of the filter paper was recorded before filtration and after drying the sample at room temperature. The  $\text{CaCO}_3$  precipitate mass was determined using the formula,

$$M_{\text{CaCO}_3} = (M_{\text{F}+\text{Material}} - M_{\text{F}}) - (M_{\text{FC}+\text{Material}} - M_{\text{FC}})$$

Wherein,  $M_{\text{F}+\text{Material}}$  indicates the combined mass of the experimental filter and retentate,  $M_{\text{F}}$  is the mass of the experimental filter alone,  $M_{\text{FC}+\text{Material}}$  represents the mass of the control filter plus retentate and  $M_{\text{FC}}$  corresponds to the mass of the control filter alone (Krishnapriya & Babu, 2015).

#### Precipitation in Agar media

The precipitation of  $\text{CaCO}_3$  in solid media was carried out according to the method described by Hammad et al., (2013), with slight modifications. Calcite Precipitation Agar (CPA) was prepared by incorporating the following components ( $\text{g mL}^{-1}$ ): nutrient broth, 2% (w/v) urea, 2.85% (w/v) calcium chloride, 0.212% (w/v) sodium bicarbonate, 1% (w/v) ammonium chloride, and 2% (w/v) bacteriological agar. To assess  $\text{CaCO}_3$  precipitation, 20  $\mu\text{L}$  of bacterial culture, with an absorbance of 0.5 at 600 nm was inoculated at the center of the CPA plate. The cultures were incubated at 30°C for 10 days, after which the plates were examined for precipitation kinetics over a 10-day period, with sampling conducted every 2 days, and its diameter was subsequently measured. A small portion of the CPA medium from the precipitation zone was carefully transferred to a clean glass slide for microscopic analysis (Hammad et al., 2013).

### Urease Activity and Urea Degradation

Urease activity was determined following the phenol-hypochlorite assay, wherein 250 mL of bacterial suspension was added to 250 mL of 0.1 M sodium phosphate buffer, followed by the addition of 500 mL of 3 M urea solution. For each sample, 2 mL of phenol nitroprusside solution was added and subsequently incubated at 50°C for 10 min. For each sample, 2 mL of phenol nitroprusside solution was added and subsequently incubated at 50°C for 10 min. The production of ammonium was measured spectrophotometrically at 626 nm to assess urease activity (Kang et al., 2016).

### Cell surface hydrophobicity and adhesion

The modified hexadecane method was used to determine cell surface hydrophobicity by examining distribution of bacterial suspensions, including both spores and vegetative cells between an aqueous and a hexadecane phase. Bacterial cells were cultured for 20 hours and were collected by centrifugation at 10,000

rpm for 10 min. The samples were washed twice and resuspended in 0.9% NaCl saline solution to an OD<sub>600</sub> of 1.0. An equal volume of n-hexadecane (2 mL) was added to the cell suspension, and the resulting two-phase system was vortexed for 30 sec to ensure uniform dispersion. Following incubation at room temperature for 10 min, the aqueous phase was separated, and its absorbance at 600 nm was determined to quantify the percentage of bacterial adhesion to n-hexadecane. The percentage of bacterial adhesion to n-hexadecane was calculated as

$$(A_0 - A_t / 1.0) \times 100$$

Wherein,  $A_0$  represents the initial absorbance of the bacterial suspension at 600 nm, while  $A_t$  absorbance of the aqueous phase (the remaining bacterial suspension in the water layer) after interaction with n-hexadecane.

The cell suspension for assessing bacterial adhesion to soil was prepared in accordance with the above-described procedure. A 1 mL volume of cell suspension was mixed with 100 mg of soil particles, followed by vortexing for 30 sec and incubation at room temperature for 10 min. The aqueous phase was removed, and its absorbance at 600 nm was recorded, and the percentage of bacterial adhesion to soil was determined using the above given formula (Kang et al., 2016).

## **Bioconsolidation Studies**

### **Bioconsolidation of soil samples**

The bioconsolidation studies were carried out using petri plates, with soil samples subjected to sieving followed by autoclaving to effectively remove any residual microbial contaminants. The bacterial suspension comprising of vegetative cells as well as spores were harvested from an overnight culture by centrifugation at 10,000 rpm for 10 min. The resulting pellet was washed twice and then resuspended in saline solution to obtain a final OD<sub>600</sub> of 0.05. Approximately 50 g of sterile soil was thoroughly mixed with 20 mL of bacterial suspension and 10 mL of a 20 g mL<sup>-1</sup> calcium chloride (CaCl<sub>2</sub>) solution. Subsequently, the mixture was spread uniformly across the surface of a Petri plate to ensure uniformity. The soil samples, supplemented with 10 mL of a 20 g mL<sup>-1</sup> calcium chloride (CaCl<sub>2</sub>) solution without bacterial suspension, served as the control. The Petri plates were incubated at 30°C for 7 days, followed by drying of the soil samples at 60°C for 24 hours. The surface pore sizes of the treated soil samples as well as untreated controls were observed (Kang et al., 2016).

### **Tightness assessment of bioconsolidated soil**

The tightness test was conducted to assess the ability of bioconsolidated sand to slow water flow. Sand samples were dried at 45°C for 24 hours to ensure the evaporation of residual moisture, followed by cooling to room temperature. Approximately 50 g of treated sand was transferred into petri plates and mounted in fixed holders. To evaluate water retention, 20 mL of water was poured onto the surface of the sand. The time taken for the first droplet to appear (retention time) was recorded. The experiment was conducted in triplicates, and the average retention time was calculated. Sand samples treated without bacterial cells served as controls for comparison (Khadim et al., 2022).

### **Water absorption analysis of bioconsolidated soil**

The water absorption characteristics of bioconsolidated and control soil were analyzed following the curing process. The samples were first dried at 45°C for 24 hours to ensure the complete removal of residual moisture. After drying, the samples were submerged in tap water for 24 hrs to achieve full saturation. The saturated specimens were initially weighed (W1), then dried at 80°C for 24 hours and re-weighed (W2). The water absorption was then calculated using the following formula (Abo-El-Enein et al., 2012)

$$\text{Water absorption (\%)} = [(W1 - W2) / W1] \times 100$$

### **Penetration analysis of bioconsolidated soil**

The penetration testing was carried out to assess the cementation strength of both bioconsolidated and control soil samples. The soil samples were subjected to a modified needle penetration test utilizing a needle with a diameter of 2.5 mm and a height of 7 cm. The penetration value corresponds to the vertical distance traveled by the needle's tip within the soil samples (Abo-El-Enein et al., 2012).

## Results and discussions

### Isolation of ureolytic bacteria

An enrichment medium was utilized for the isolation of ureolytic bacteria, with 36 hours incubation at 28°C to promote proliferation. The thirty-four bacterial isolates obtained were distinguished by its unique colony morphology and was further evaluated for ureolytic activity on nutrient agar enriched with 8% urea. The isolates exhibiting the highest ureolytic activity, as indicated by a rapid color change to pink within the first 24 hours of incubation at 28°C, detected using phenolphthalein as a pH indicator. The color shift was attributed to the release of ammonia ( $\text{NH}_3/\text{NH}_4^+$ ) released through urease-mediated hydrolysis and this subsequently elevated the pH of the medium. A single bacterial isolate exhibiting the most substantial and rapid development of pink halos was selected for further molecular analysis (Figure 1).

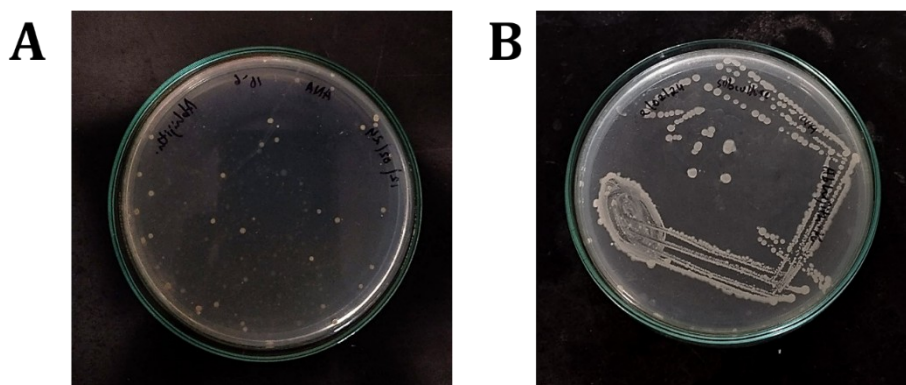


**Figure 1.** Bacteria isolated from soil. A. Spread culture technique plate. B. Pure culture maintenance.

### Molecular characterization of the urease producing bacteria

The retrieved sequences were subjected to sequence alignment NCBI GenBank database using the BLAST tool. The homology analysis confirmed the presence of the *Bacillus* genus, exhibiting a 98% sequence identity to *Bacillus tequilensis* strain MITCV1 (MG461176.1). Subsequently, the isolate's sequence was deposited in the GenBank database receiving the accession number PP783866.1 and was designated as *Bacillus tequilensis* strain AK1.

### Assessment of Calcium Carbonate Precipitation

#### Precipitation in broth Media

The precipitation of calcium carbonate ( $\text{CaCO}_3$ ) by *Bacillus tequilensis* strain AK1 was assessed, with white calcite precipitate first appearing on Day 10 in B4 medium and its density increasing progressively during the incubation (Figure 2A). The calcite precipitates were collected and quantified at regular 2-day intervals over the course of the incubation period. The  $\text{CaCO}_3$  deposition gradually increased over the course of the incubation, from 7.20 mg mL<sup>-1</sup> on Day 10 to 10.35 mg mL<sup>-1</sup> on Day 12, 13.60 mg mL<sup>-1</sup> on Day 14, 17.10 mg mL<sup>-1</sup> on Day 16, 20.50 mg mL<sup>-1</sup> on Day 18, and reached a maximum of 23.00 mg mL<sup>-1</sup> on Day 20. These results, as shown in Figure 3A highlight the potential of *Bacillus tequilensis* strain AK1 for sustained and efficient calcium carbonate precipitation over the incubation period. Calcite precipitation rates reported in previous studies include 15.3 mg mL<sup>-1</sup> in 5 days (Kang et al., 2016), 19.3 mg mL<sup>-1</sup> in 7 days (Khadim et al., 2022), 1.85 mg mL<sup>-1</sup> in 10 days (Andreolli et al., 2011), 65 mg mL<sup>-1</sup> in 7 days, and 1.8 g mL<sup>-1</sup> in 2 days (Yuan 2020), 38 g mL<sup>-1</sup> in 2 days (Nayanthara et al., 2019), 4g mL<sup>-1</sup> in 7 days (Dikshit et al., 2020), 0.3g mL<sup>-1</sup> in 12 hours (Ma et al., 2020) along with 40.1 g mL<sup>-1</sup> in 12 days (Peng & Liu, 2019).

#### Precipitation in Agar media

The  $\text{CaCO}_3$  precipitation potential of *Bacillus tequilensis* strain AK1 was further investigated calcite precipitation agar (CPA). CPA functions as a solid medium for the detection of bacteria capable of promoting calcium carbonate precipitation via ureolytic activity. The formation of  $\text{CaCO}_3$  on CPA manifested as a white precipitate localized within the growth zone and its peripheral region (Figure 2B). The measurements of the precipitation zone diameters performed over a 10-day period demonstrated a consistent increase in size, as represented in Figure 3B.

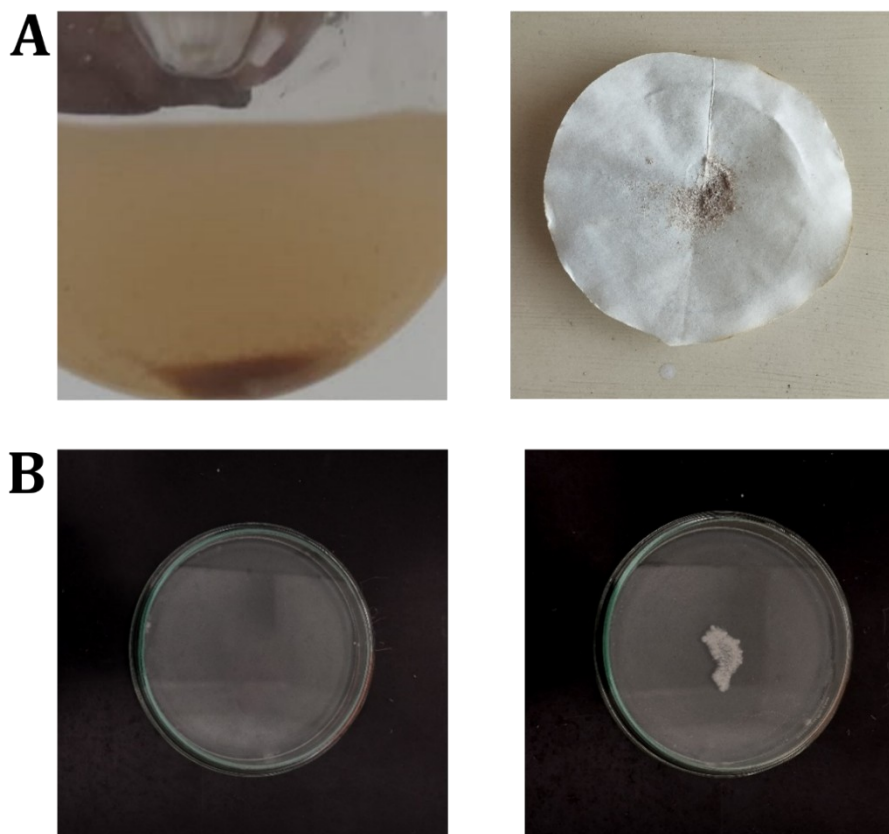


**Figure 2.** CaCO<sub>3</sub> precipitation in broth and agar state. A. Precipitate seen at bottom of the conical flask and weighed precipitate filtrate from broth medium, B: Control plate and precipitation exhibited by *Bacillus tequilensis* strain AK1 on CPA media.

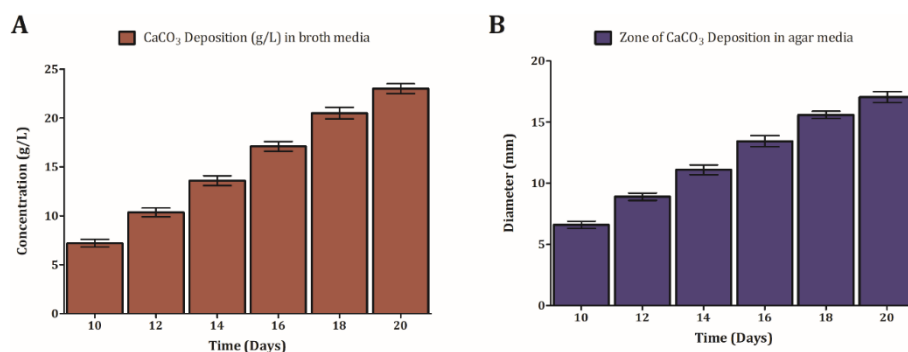


**Figure 3.** CaCO<sub>3</sub> deposition rate in broth and agar state. A. Concentration of CaCO<sub>3</sub> deposition by *Bacillus tequilensis* strain AK1 in broth medium B. Zone of CaCO<sub>3</sub> deposition by *Bacillus tequilensis* strain AK1 in CPA media.

The largest precipitation zone of CaCO<sub>3</sub> with a diameter of 17.05 mm, was observed on Day 20, with subsequent measurements of 15.60 mm on Day 18, 13.40 mm on Day 16, and 11.10 mm on Day 14. The smallest zones were observed earlier in the incubation period, with diameters of 6.60 mm and 8.90 mm observed on Days 10 and 12, respectively. Therefore, the precipitation on CPA exhibited a progressive increase, thereby indicating the potential of *Bacillus tequilensis* AK1 in facilitating biocementation.

### Urease activity and urea degradation

The urease activity and urea degradation capabilities of *Bacillus tequilensis* AK1 were measured spectrophotometrically and the results demonstrated a steady rise in urea degradation and the concomitant production of calcite over time (Figure 4). Following 24 hours of incubation, the level of urea degradation reached 200  $\mu\text{mol mL}^{-1}$  corresponding to a mean calcite production of 8.0  $\text{mg mL}^{-1}$ , while at 48 hours, the degradation level of urea had elevated to 310  $\mu\text{mol mL}^{-1}$  with a corresponding mean calcite production of 12.4  $\text{mg mL}^{-1}$ .

The optimal urease activity and calcite formation were recorded at 72 hours with urea degradation of 400  $\mu\text{mol mL}^{-1}$  and a corresponding calcite production of 14.7  $\text{mg mL}^{-1}$ . Subsequently, the rates of urea degradation and calcite formation plateaued showing no further substantial changes. This interpretation is



supported by the peak urease activity at 72 hours, aligning with observations by Nayanthara et al., 2019, who reported that urease production is closely associated with the exponential growth phase in ureolytic bacteria (Nayanthara et al., 2019). Similarly, Dhama et al. 2017 reported peak urease activity at 96 hours under high-nutrient enrichment, highlighting how nutrient availability influences enzyme expression (Dhama et al. 2017). Likewise, Gowthaman et al. (2019) reported that biomass concentration increased initially up to 48–96 hours and remained relatively stable thereafter, highlighting how microbial growth dynamics plateau over time under given conditions (Gowthaman et al., 2019). The urea degradation was  $410 \mu\text{mol mL}^{-1}$  at 96 hours with calcite production of  $15.1 \text{ mg mL}^{-1}$  and the maximum values were attained at 120 hours with urea degradation increasing to  $415 \mu\text{mol mL}^{-1}$  and calcite production peaking at  $15.3 \text{ mg mL}^{-1}$ . These results corroborate the findings of Stahler et al., (2005) (Stähler et al., 2005) which showed that urea hydrolysis led to the accumulation of  $\text{HCO}_3^-$  and  $\text{NH}_4^+$ , thereby facilitating carbonate metabolism.

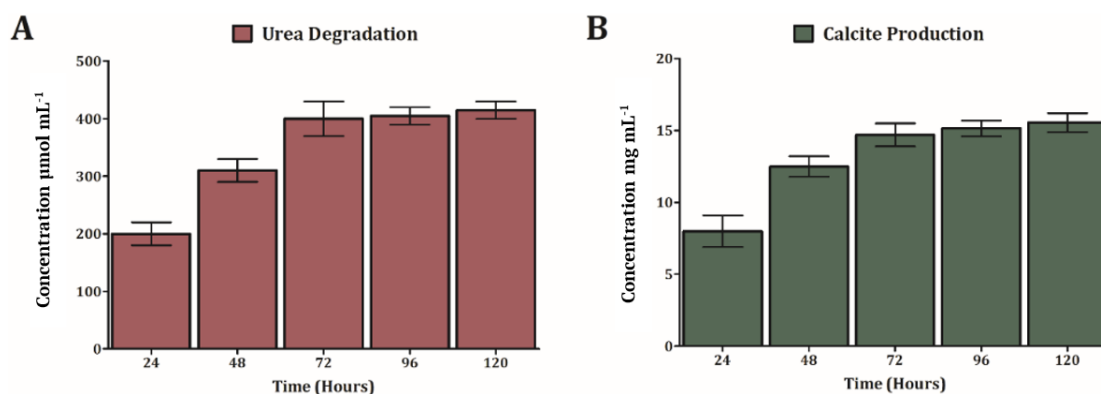


**Figure 4.** Urea degradation and Urease activity of *Bacillus tequilensis* strain AK1. A. Evaluation of the level of urea degradation by *Bacillus tequilensis* strain AK1. B. Assessment of Calcite production by *Bacillus tequilensis* strain AK1.

### Cell surface hydrophobicity and adhesion

The water–hexadecane distribution assay demonstrated that vegetative cells were predominantly hydrophilic with only 19% affinity for hexadecane, whereas spores displayed strong hydrophobic tendency with an 84.5% affinity for hexadecane (Figure 5A). The subsequent assessment of the critical surface tension (CST) values for soils treated with vegetative cells and spores revealed that spores exhibited significantly higher adhesion (55%), whereas vegetative cells showed only 10% adhesion (Figure 5B).

The observed hydrophobic nature of spores (84.5%) and the elevated adhesion rate (55%) are consistent work of Wiencek et al. (1990) (Wiencek et al. 1990), who attributed the enhanced spore hydrophobicity to the protein-rich outer coats and exosporia. Jacobs et al., (2007) (Jacobs et al., 2007) established a positive correlation between hydrophobicity and soil adhesion, emphasizing its critical role in facilitating bioconsolidation processes. Achal et al., (2009) demonstrated that effective bacterial adhesion and distribution play a key role in promoting calcite formation, thereby ensuring the efficient stabilization of soil. Kang et al. 2015 also reported through water–hexadecane distribution analysis that vegetative cells were hydrophilic (24%), whereas spores were hydrophobic (80%) (Kang et al. 2015).

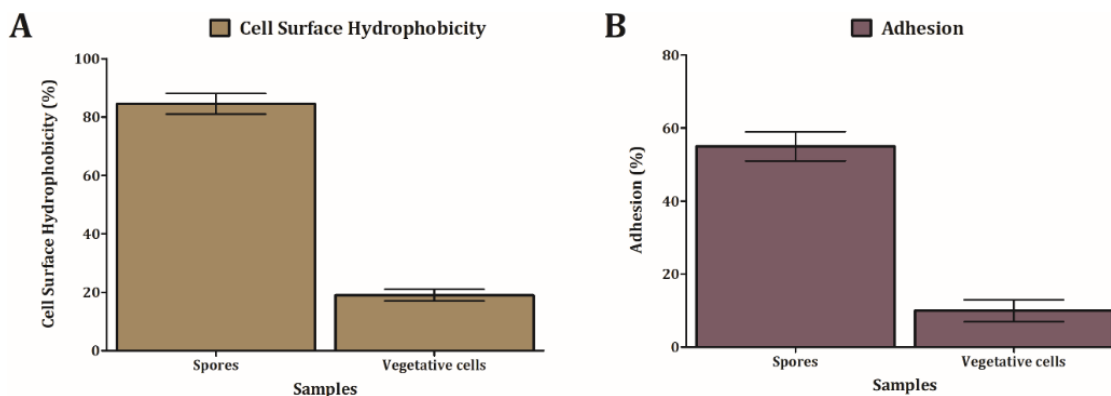


**Figure 5.** Cell surface hydrophobicity and adhesion A. Cell surface hydrophobicity determination of *Bacillus tequilensis* strain AK1. B. Adhesion capacity *Bacillus tequilensis* strain AK1.

## Bioconsolidation studies

### Bioconsolidation of soil samples

The present study involved examination of soil dynamics by directly applying *Bacillus tequilensis* strain AK1 to the soil. A higher porosity was observed in the control samples when compared to the treated samples (Figure 6). This phenomenon may be attributed to the calcite precipitation induced by the application of *Bacillus tequilensis* strain AK1.

The bioconsolidation effects observed in treated with *Bacillus tequilensis* strain AK1 are in accordance with prior studies that emphasize the importance of microbial size and pore structure characteristics in enhancing soil stabilization (Achal et al., 2009). The reduced porosity in the treated samples is likely due to calcite precipitation, which is facilitated by spore germination and contributes to the cementation of soil particles (Setlow, 2010; Madigan et al., 2003). Spores exhibit resistance to extreme environmental conditions and are able to germinate under favorable conditions to produce vegetative cells that facilitate the precipitation of calcite (Paidhungat & Setlow, 2001).

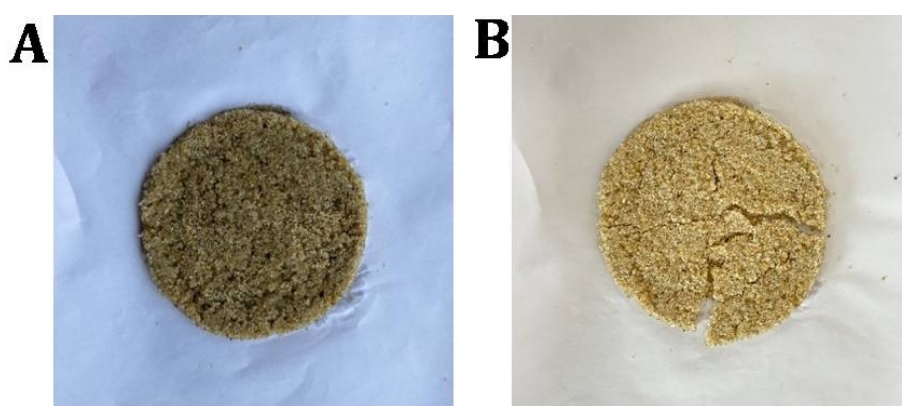


**Figure 6.** Bioconsolidation of soil samples A. Bioconsolidation of the soil sample due to the production of Calcium carbonate by *Bacillus tequilensis* strain AK1. B. Control soil sample.

### Tightness assessment of bioconsolidated soil

The retention time is quantified as the interval between the introduction of water and the emergence of the initial drop. As depicted in Figure 7A, the control samples exhibited a substantially lower average retention time of 15 sec, whereas the bio-consolidated soil samples recorded a significantly higher retention time of 164 sec. The considerable elevation in retention time for the bio-consolidated soil samples (164 sec) relative to the control samples (15 sec) indicates an enhanced resistance to water flow, potentially due to the deposition of calcium carbonate. These results are consistent with existing research that have shown that bioconsolidation modifies sand permeability and enhances its structural integrity through the generation of plugging materials (Achal et al., 2009). The observed variations in retention time are likely a consequence of calcium carbonate crystal size, with smaller crystals contributing to improved plugging efficiency, thereby prolonging retention time.

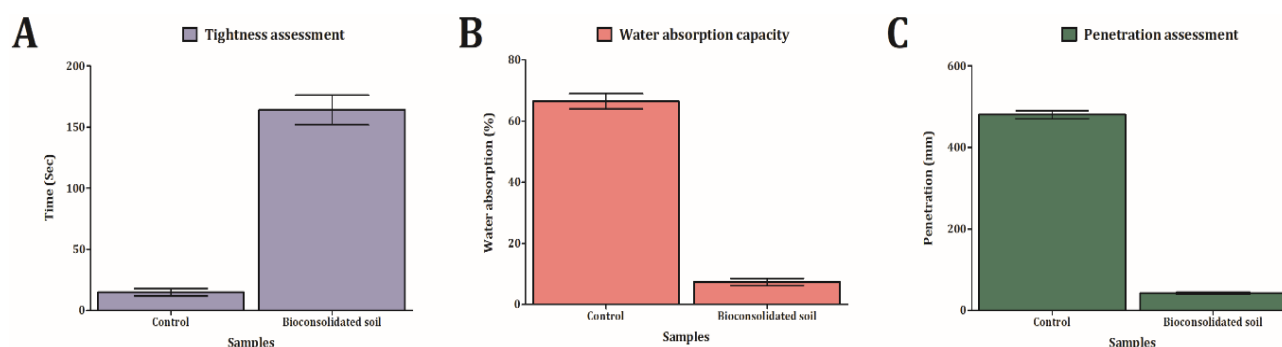


**Figure 7.** Characterization of the bioconsolidation of soil sample A. A. Tightness assessment of bioconsolidated soil. B. Water absorption analysis of bioconsolidated soil. C. Penetration analysis of bioconsolidated soil.



### Water absorption analysis of bioconsolidated soil

The water retention properties of bioconsolidated soil treated with *Bacillus tequilensis* strain AK1 and the corresponding control sample is represented in Figure 7B. The water absorption analysis revealed a pronounced reduction in the bioconsolidated soil's absorption capacity (7.4%) relative to the control soil (66.5%), indicating efficient pore filling through calcium carbonate precipitation. This is consistent with existing literature demonstrating that increased precipitation of calcium carbonate effectively reduces open porosity in the sand, thereby minimizing its water absorption capacity (Abo-El-Enein et al., 2009). This observation aligns with findings by Sarda et al. (2009), who reported that water absorption in control bricks was 24.97%, while treatment with nutrient broth (NB) and brain heart infusion (BHI) media led to significant reductions to 21.47% and 13.84%, respectively corresponding to 14.1% and 44.5% decreases further supporting the role of microbial treatment in reducing material porosity through calcium carbonate precipitation (Sarda et al., 2009).

### Penetration analysis of bioconsolidated soil

The penetration values obtained from the needle penetration tests for both control and bioconsolidated samples are depicted in Figure 7C. The penetration distance for no-cell control samples was 483 mm, whereas the bioconsolidated samples revealed a considerably reduced distance of 43 mm. The substantial reduction in penetration distance observed in the bioconsolidated samples (43 mm) relative to the control samples (483 mm) signifies the increased soil hardness and cementation, which can be attributed to the calcium carbonate deposition. The microbial-driven process of calcite precipitation facilitates development of calcite bridges between soil particles, thereby enhancing the overall strength and degree of consolidation. The present findings are consistent with previous studies, that have shown the addition of calcium carbonate decreases porosity and enhances soil stability through particle aggregation (Khadim et al., 2022).

## Conclusion

This study highlights the promising potential of *Bacillus tequilensis* strain AK1 for effective bioconsolidation of soil and sand via microbially induced calcium carbonate precipitation (MICP). The bacterium demonstrated exhibited elevated urease activity that facilitated substantial calcium carbonate deposition and enhanced soil stability by lowering porosity, increasing hardness, and enhancing water flow resistance. The findings emphasize the strain's capacity to induce calcite bridge formation between soil particles, thus improving the structural stability of the soil. These findings highlight the potential of MICP as a sustainable, eco-friendly solution, with future research efforts aimed at scaling the process and optimizing its long-term stability.

## Acknowledgment

The authors would like to express sincerest gratitude to the Institutions, Hindusthan College of Arts & Science, Dr. NGP Arts & Science College, Coimbatore, Tamil Nadu, India for providing all the resources to carry out the work. The authors are thankful to the technicians from Hindusthan College of Arts & Science, and Dr. NGP Arts & Science College for their consistent support in execution of the experiments.

## References

- Abo-El-Enein, S. A., Ali, A. H., Talkhan, F. N., & Abdel-Gawwad, H. A. (2012). Utilization of microbial induced calcite precipitation for sand consolidation and mortar crack remediation. *HBRC Journal*, 8(3), 185–192. <https://doi.org/10.1016/j.hbrcj.2012.10.002>
- Achal, V., Mukherjee, A., Basu, P. C., & Reddy, M. S. (2009). Strain improvement of *Sporosarcina pasteurii* for enhanced urease and calcite production. *Journal of Industrial Microbiology & Biotechnology*, 36(9), 981–988. <https://doi.org/10.1007/s10295-009-0612-0>
- Al-Thawadi, S., & Cord-Ruwisch, R. (2012). Calcium carbonate crystals formation by ureolytic bacteria isolated from Australian soil and sludge. *Journal of Advanced Science and Engineering Research*, 2(1), 12–26. <https://doi.org/10.15515/jaser.2012.21002>
- Andreolli, M., Lampis, S., Zenaro, E., Salkinoja-Salonen, M., & Vallini, G. (2011). *Burkholderia fungorum* DBT1: A promising bacterial strain for bioremediation of PAHs-contaminated soils. *FEMS Microbiology Letters*, 319(1), 11–18. <https://doi.org/10.1111/j.1574-6968.2011.02298.x>

- DeJong, T. T., Mortensen, B. M., Martinez, B. C., & Nelson, D. C. (2010). Bio-mediated soil improvement. *Ecological Engineering*, *36*(2), 197–210. <https://doi.org/10.1016/j.ecoleng.2009.02.008>
- Dhami, N. K., Alsubhi, W. R., Watkin, E., & Mukherjee, A. (2017). Bacterial community dynamics and biocement formation during stimulation and augmentation: Implications for soil consolidation. *Frontiers in Microbiology*, *8*, 1267. <https://doi.org/10.3389/fmicb.2017.01267>
- Dhami, N. K., Reddy, M. S., & Mukherjee, A. (2013). Biomineralization of calcium carbonate polymorphs by the bacterial strains isolated from calcareous sites. *Journal of Microbiology and Biotechnology*, *23*(5), 707–714. <https://doi.org/10.4014/jmb.1301.01007>
- Dikshit, R., Jain, A., Dey, A., & Kumar, A. (2020). Microbially induced calcite precipitation using *Bacillus velezensis* with guar gum. *PLOS ONE*, *15*(8), e0236745. <https://doi.org/10.1371/journal.pone.0236745>
- Ghosh, T., Bhaduri, S., Montemagno, C., & Kumar, A. (2019). *Sporosarcina pasteurii* can form nanoscale calcium carbonate crystals on cell surface. *PLoS One*, *14*(8), e0210339. <https://doi.org/10.1371/journal.pone.0210339>
- Gowthaman, S., Iki, T., Nakashima, K., Ebina, K., & Kawasaki, S. (2019). Feasibility study for slope soil stabilization by microbial induced carbonate precipitation (MICP) using indigenous bacteria isolated from cold subarctic region. *SN Applied Sciences*, *1*(9), 1–16. <https://doi.org/10.1007/s42452-019-1508-y>
- Hammad, I. A., Talkhan, F. N., & Zoheir, A. E. (2013). Urease activity and induction of calcium carbonate precipitation by *Sporosarcina pasteurii* NCIMB 8841. *Journal of Applied Sciences Research*, *9*(5), 1525–1533. <https://doi.org/10.9734/JASR/2013/3140>
- Hammes, F., & Verstraete, W. (2002). Key roles of pH and calcium metabolism in microbial carbonate precipitation. *Reviews in Environmental Science and Biotechnology*, *1*(1), 3–7. <https://doi.org/10.1023/A:1015135629155>
- Jacobs, A., Lafolie, F., Herry, J. M., & Debroux, M. (2007). Kinetic adhesion of bacterial cells to sand: Cell surface properties and adhesion rate. *Colloids and Surfaces B: Biointerfaces*, *59*(1), 35–45. <https://doi.org/10.1016/j.colsurfb.2007.03.002>
- Kang, C. H., Kwon, Y. J., & So, J. S. (2016). Soil bioconsolidation through microbially induced calcite precipitation by *Lysinibacillus sphaericus* WJ-8. *Geomicrobiology Journal*, *33*(5), 473–478. <https://doi.org/10.1080/01490451.2015.1137600>
- Khadim, H. J., Ebrahim, S. E., & Ammai, S. H. (2022). Sand bioconsolidation/biosolidification by microbially induced carbonate precipitation using ureolytic bacteria. *AIP Conference Proceedings*, *2398*(1), 1–6. <https://doi.org/10.1063/5.0089070>
- Krishnapriya, S., & Babu, D. V. (2015). Isolation and identification of bacteria to improve the strength of concrete. *Microbiological Research*, *174*, 48–55. <https://doi.org/10.1016/j.micres.2015.02.003>
- Ma, L., Pang, A. P., Luo, Y., Lu, X., & Lin, F. (2020). Beneficial factors for biomineralization by ureolytic bacterium *Sporosarcina pasteurii*. *Microbial Cell Factories*, *19*(1), 1–12. <https://doi.org/10.1186/s12934-020-1281-z>
- Madigan, M. T., Martinko, J. M., & Parker, J. (2003). *Brock biology of microorganisms* (10th ed.). Pearson Education Inc.
- Mitchell, A. C., & Ferris, F. G. (2005). The coprecipitation of Sr into calcite precipitates induced by bacterial ureolysis in artificial groundwater: Temperature and kinetic dependence. *Geochimica et Cosmochimica Acta*, *69*(17), 4199–4210. <https://doi.org/10.1016/j.gca.2005.04.010>
- Nayanthara, P. G. N., Dassanayake, A. B. N., Nakashima, K., & Kawasaki, S. (2019). Biocementation of Sri Lankan beach sand using locally isolated bacteria: A baseline study on the effect of segregated culture media. *GEOMATE Journal*, *17*(63), 55–62. <https://doi.org/10.21660/2019.63.8238>
- Paidhungat, M., & Setlow, P. (2001). Spore germination and outgrowth. In P. J. Schaeffer (Ed.), *Bacillus subtilis and its closest relatives: From genes to cells* (pp. 537–548). ASM Press.
- Park, I. S., & Hausinger, R. P. (1995). Requirement of carbon dioxide for in vitro assembly of the urease nickel metallocenter. *Science*, *267*(5195), 1156–1158. <https://doi.org/10.1126/science.267.5195.1156>
- Peng, J., & Liu, Z. (2019). Influence of temperature on microbially induced calcium carbonate precipitation for soil treatment. *PLoS One*, *14*(3), e0218396. <https://doi.org/10.1371/journal.pone.0218396>

- Qian, C., Wang, R., Cheng, L., & Wang, J. (2010). Theory of microbial carbonate precipitation and its application in restoration of cement-based materials defects. *Chinese Journal of Chemistry*, 28(7), 847–857. <https://doi.org/10.1002/cjoc.201090126>
- Sarda, D., Choonia, H. S., Sarode, D. D., & Lele, S. S. (2009). Biocalcification by *Bacillus pasteurii* urease: a novel application. *Journal of Industrial Microbiology and Biotechnology*, 36(8), 1111–1115. <https://doi.org/10.1007/s10295-009-0581-4>
- Setlow, P. (2010). Resistance of bacterial spores. In P. Setlow (Ed.), *Bacterial stress responses* (pp. 319–332). Springer. [https://doi.org/10.1007/978-1-4419-1673-0\\_19](https://doi.org/10.1007/978-1-4419-1673-0_19)
- Stähler, F. N., Ganter, L., Lederer, K., Kist, M., & Bereswill, S. (2005). Mutational analysis of the *Helicobacter pylori* carbonic anhydrases. *FEMS Immunology & Medical Microbiology*, 44(2), 183–189. <https://doi.org/10.1016/j.femsim.2005.03.013>
- Sujatha, P., Kumar, B. N., & Kalarani, V. (2012). Isolation, characterization, and molecular identification of bacteria from tannery effluent using 16S rRNA sequencing. *International Journal of Environmental Sciences*, 3(1), 1–8. <https://doi.org/10.6088/ijes.2012030101001>
- Vekariya, M. S., & Pitroda, J. (2013). Bacterial concrete: New era for construction industry. *International Journal of Engineering Trends and Technology*, 4(11), 4128–4137. <https://doi.org/10.14445/22315381/IJETT-V4P234>
- Wang, J. Y., Soens, H., Verstraete, W., & De Belie, N. (2014). Self-healing concrete by use of microencapsulated bacterial spores. *Cement and Concrete Research*, 56, 139–152. <https://doi.org/10.1016/j.cemconres.2013.11.004>
- Weiner, S. (2008). Biomineralization: A structural perspective. *Journal of Structural Biology*, 163(2), 229–234. <https://doi.org/10.1016/j.jsb.2008.02.006>
- Wiencek, K. M., Klapes, N. A., & Foegeding, P. M. (1990). Hydrophobicity of *Bacillus* and *Clostridium* spores. *Applied and Environmental Microbiology*, 56(8), 2600–2605. <https://doi.org/10.1128/aem.56.8.2600-2605.1990>
- Yuan, L. (2020). Influencing factors and formation mechanism of CaCO<sub>3</sub> precipitation induced by microbial carbonic anhydrase. *Biotechnology Bulletin*, 36, 79. <https://doi.org/10.1016/j.biotech.2020.05.003>